Journal of Statistical Physics, Vol. 72, Nos. 1/2, 1993

Phase Transitions in an Exactly Soluble One-Dimensional Exclusion Process

G. Schütz[1] **and E. Domany**[2]

Received December 14, 1992

We consider an exclusion process with particles injected with rate α at the origin and removed with rate β at the right boundary of a one-dimensional chain of sites. The particles are allowed to hop onto unoccupied sites, to the right only. For the special case of $\alpha=\beta=1$ the model was solved previously by Derrida *et al.* Here we extend the solution to general α, β. The phase diagram obtained from our exact solution differs from the one predicted by the mean-field approximation.

KEY WORDS: Asymmetric exclusion process; steady state; boundary-induced phase transitions.

1. INTRODUCTION

One-dimensional asymmetric exclusion models[1] are of interest for various reasons. They are closely related to vertex models,[2] growth models,[3] and, in the continuum limit, the KPZ equation[4] and the noisy Burgers's equation.

Various types of phase transitions occur as a consequence of the interplay of particle transport with a localized defect or inhomogeneity. Suitably chosen boundary conditions can represent the effect of such a defect in an otherwise homogeneous system. Such transitions have been the focus of many recent studies.[1,5–9] Some of these models could be solved exactly and allow for a detailed study of their steady-state properties, such as the density profile or density correlations.[1,7–9]

Totally asymmetric simple-exclusion models with nearest neighbor hopping can be divided into four classes according to the dynamics

[1] Department of Physics, Weizmann Institute, Rehovot 76100, Israel.
[2] Department of Electronics, Weizmann Institute, Rehovot 76100, Israel.

(sequential or parallel) and the choice of boundary conditions (open or periodic). In all these models each lattice site i in a chain of N sites is either occupied by a single particle ($\tau_i = 1$) or empty ($\tau_i = 0$) and a particle can hop to the neighboring site in one direction if this site is empty.[3] By convention, we choose the direction of hopping as to the right. The dynamics can be chosen either sequential[1,5,6,8] or parallel.[2,7,9] In the case of sequential dynamics, which we study in this paper, particles jump independently and randomly in each time step according to the following rules: At each time step $t \to t+1$ one chooses at random one pair of sites $(i, i+1)$ with $1 \leqslant i \leqslant N-1$. If there is a particle on site i and site $i+1$ is empty, then the particle will jump from i to $i+1$. All other configurations do not change, i.e.,

$$\begin{aligned} \tau_i(t+1) &= \tau_i(t)\, \tau_{i+1}(t) \\ \tau_{i+1}(t+1) &= \tau_{i+1}(t) + [1 - \tau_{i+1}(t)]\, \tau_i(t) \end{aligned} \tag{1.1}$$

In the case of parallel updating the lattice is divided into neighboring pairs of sites and some stochastic hopping rules are applied in parallel to each pair in a first half time step. In the second half time step the pairs are shifted by one lattice unit and the same rules are applied again.[2,7,9] Both models can be defined with either periodic or open boundary conditions. When periodic boundary conditions are used, a nontrivial phase diagram can be observed by introducing, for example, a single defect.[6,7] With open boundary conditions particles are injected with rate α at the left boundary (which we shall call the *origin*) and absorbed with rate β at the right *boundary*.[1,5,8,9] Injection and absorption are implemented in the following way: when one considers the pair (0, 1), where site 0 represents the origin, then the occupation number $\tau_1(t+1)$ of site 1 at time $t+1$ is given by

$$\begin{aligned} \tau_1(t+1) &= 1 \qquad \text{with probability } \tau_1(t) + \alpha[1 - \tau_1(t)] \\ \tau_1(t+1) &= 0 \qquad \text{with probability } (1-\alpha)[1 - \tau_1(t)] \end{aligned} \tag{1.2}$$

On the other hand, considering the pair $(N, N+1)$, where site $N+1$ represents the (right) boundary, the occupation number $\tau_N(t+1)$ at site N after one time step is

$$\begin{aligned} \tau_N(t+1) &= 1 \qquad \text{with probability } (1-\beta)\, \tau_N(t) \\ \tau_N(t+1) &= 0 \qquad \text{with probability } 1 - (1-\beta)\, \tau_N(t) \end{aligned} \tag{1.3}$$

[3] A model with two different kinds of particles and nearest neighbor hopping has been studied in ref. 10, and a simple-exclusion model where particles can hop over several lattice sites in each time step is discussed in ref. 11.

The model defined by Eqs. (1.1)–(1.3) can be viewed as a homogeneous system connected to a reservoir of fixed particle density α at the origin and fixed density $1-\beta$ at the boundary.

The model with parallel dynamics and periodic boundary conditions with a defect[7] was solved by the Bethe ansatz. Recently some steady-state properties of the model with parallel dynamics and open boundary conditions were also found.[9] The Bethe ansatz was used also to solve the model with sequential updating (1.1) and translationally invariant periodic boundary conditions without defect.[12] The case of sequential dynamics with open boundary conditions was studied by Krug[5] and by Derrida *et al.*[1]

Krug studied numerically the steady-state behavior of this model on the line $\beta=1$ (Fig. 1). He found, at $\alpha=1/2$, a phase transition and an associated diverging length scale.[5] For $\alpha<1/2$ he found an exponential decay of the profile to its bulk value with increasing distance r from the boundary, while for $\alpha>1/2$ the profile decayed as $r^{-1/2}$. Derrida *et al.*[1] expressed the exact steady state and the steady-state density distribution for arbitrary α and β in terms of recursion relations [Eqs. (2.9)–(2.11) below]. These recursions were solved explicitly only for $\alpha=\beta=1$. For this

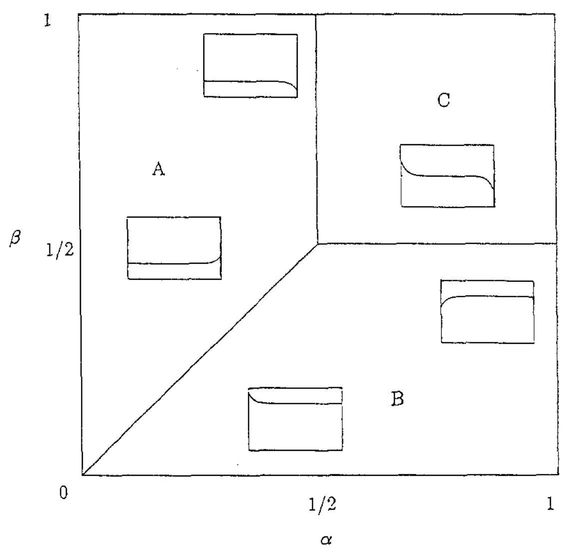

Fig. 1. Mean-field phase diagram of the model in the α–β plane as obtained in ref. 1. Region A is the low-density phase, region B the high-density phase, and region C the maximal current phase. The phases are separated by the curves $\alpha=\beta<1/2$; $\alpha=1/2$, $\beta>1/2$; and $\beta=1/2$, $\alpha>1/2$, respectively. The sign of the slope of the density profile (as shown in the insets) changes when the line $\alpha=1-\beta$ is crossed. Note that this is *not* a phase transition line.

case they showed that the density profile approaches algebraically its bulk value $\rho_{\text{bulk}} = 1/2$ with increasing distance x from the origin, $\rho - 1/2 \sim x^{-1/2}$. The same behavior characterizes the approach of ρ_{bulk} from below as $r^{-1/2}$, with increasing distance r from the boundary, confirming the numerical result of Krug.

The phase diagram in the whole α–β plane was obtained in ref. 1 by a *mean-field* calculation. Three phases were identified (Fig. 1). In a low-density phase A, found for $\alpha < \beta$ and $\alpha < 1/2$, the density profile approaches $\rho_{\text{bulk}} = \alpha$ exponentially with r. This supports Krug's observation of an exponential behavior for $\beta = 1$, $\alpha < 1/2$. A high-density phase B was found for $\alpha > \beta$ and $\beta < 1/2$, which is related to the low-density phase by a particle–hole symmetry. Here the profile approaches $\rho_{\text{bulk}} = 1 - \beta$ exponentially with x, the distance from the origin. Finally, for α, $\beta > 1/2$ the system is in the maximal current phase C. In this phase mean field predicts a power law for the profile, with exponent $\kappa = 1$, whereas the exact result[1] yields $\kappa = 1/2$.

Here we present the exact solution to the recursion relations giving the steady state and the density profile for arbitrary values for α and β. We show that the phase diagram has a richer structure than that predicted by mean field. In particular, we show that there is a phase transition with an associated diverging length scale along the two lines, $\alpha = 1/2$ and $\beta = 1/2$, dividing both the low-density phase and the high-density phase found in the mean-field calculation into two different phases. In the low-density phase A_{I} defined by $\alpha < \beta < 1/2$ the profile is exponential, as predicted by the mean-field calculation. The situation is different, however, in the low-density phase A_{II} defined by $\alpha < 1/2$ and $\beta > 1/2$; there the profile approaches $\rho_{\text{bulk}} = \alpha$ as $r^{-3/2} \exp(-r/\xi)$ for $r \gg 1$. This was expected neither from the mean-field approach nor from the numerical results of Krug.

The paper is organized as follows. In Section 2 we present the recursion relations obtained in ref. 1 and give an exact solution for arbitrary α and β. In Section 3 we draw some conclusions from these results and derive the exact phase diagram. Then we study the density profile in the various phases for large systems (Section 4) and in Section 5 we discuss in detail the various phase transitions that were identified.

2. EXACT SOLUTION OF THE RECURSION RELATIONS

The steady state of the model defined in Eqs. (1)–(3) is given in terms of the quantities $P_N(\tau_1, \tau_2,..., \tau_N)$, which are the probabilities of finding the specific configuration of particles represented by the occupation numbers $(\tau_1, \tau_2,..., \tau_N)$ on the chain with N sites. It turns out to be more convenient to work with unnormalized probabilities $f_N(\tau_1, \tau_2,..., \tau_N)$ related to $P_N(\tau_1, \tau_2,..., \tau_N)$ by

$$P_N(\tau_1, \tau_2,..., \tau_N) = f_N(\tau_1, \tau_2,..., \tau_N)/Z_N \tag{2.1}$$

where

$$Z_N = \sum_{\tau_1=0,1} \cdots \sum_{\tau_N=0,1} f_N(\tau_1, \tau_2,..., \tau_N) \tag{2.2}$$

As shown in ref. 1, all the $f_N(\tau_1, \tau_2,..., \tau_N)$ can be obtained recursively from the corresponding quantities in a system with $N-1$ sites [Eqs. (8) and (9) of ref. 1]. Here we are interested only in the average occupation number $\langle \tau_i \rangle_N$ of site i in a system of length N, given by

$$\langle \tau_i \rangle = T_{N,i}/Z_N \tag{2.3}$$

with

$$T_{N,i} = \sum_{\tau_1=0,1} \cdots \sum_{\tau_N=0,1} \tau_i f_N(\tau_1, \tau_2,..., \tau_N) \tag{2.4}$$

The normalization Z_N and the unnormalized particle density $T_{N,i}$ can be computed from the quantities

$$Y_{N,K} = \sum_{\tau_1=0,1} \cdots \sum_{\tau_N=0,1} (1-\tau_N)(1-\tau_{N-1}) \cdots (1-\tau_K) f_N(\tau_1, \tau_2,..., \tau_N) \tag{2.5}$$

and

$$X^p_{N,K} = \sum_{\tau_1=0,1} \cdots \sum_{\tau_N=0,1} (1-\tau_N) \cdots (1-\tau_K)\, \tau_p f_N(\tau_1, \tau_2,..., \tau_N) \tag{2.6}$$

by defining

$$Y_{N,N+1} = Z_N \tag{2.7}$$

and

$$X^p_{N,N+1} = T_{N,p} \tag{2.8}$$

[Note that we made a slight change in notation as compared to ref. 1. There the quantities $Y_{N,K}$ were denoted $Y_N(K)$ and the quantities $X^p_{N,K}$ were denoted $X_N(K, p)$.]

The reason for the introduction of $Y_{N,K}$ for $1 \leqslant K \leqslant N+1$ and $X^p_{N,K}$ for

$p+1 \leqslant K \leqslant N+1$ is that they can be obtained from the following closed recursions[1]:

$$\begin{aligned} Y_{N,1} &= \beta Y_{N-1,1} \\ Y_{N,K} &= Y_{N,K-1} + \alpha\beta Y_{N-1,K} \qquad \text{for} \quad 2 \leqslant K \leqslant N \\ Y_{N,N+1} &= Y_{N,N} + \alpha Y_{N-1,N} \end{aligned} \tag{2.9}$$

with the initial condition

$$\begin{aligned} Y_{1,1} &= \beta \\ Y_{1,2} &= \alpha + \beta \end{aligned} \tag{2.10}$$

These recursions can be simplified somewhat by extending the range of definition of K to $1 \leqslant K \leqslant N+2$. If we set $K = N+1$ in the second of Eqs. (2.9), the resulting equation is precisely the third of (2.9), provided we use the extended definition $Y_{N-1,N+1} = \beta^{-1} Y_{N-1,N}$ for $\beta \neq 0$. Similarly, Eqs. (2.10) become a consequence of (2.9) by redefining the initial condition as $Y_{0,1} = 1$. These extensions of the definitions of the quantities $Y_{N,K}$ are useful in some of the calculations presented below.

Once the $Y_{N,K}$ are determined, the $X^p_{N,K}$ can be obtained from the recursion relations[1]

$$\begin{aligned} X^p_{N,K} &= X^p_{N,K-1} + \alpha\beta X^p_{N-1,K} \qquad \text{for} \quad p+2 \leqslant K \leqslant N \\ X^p_{N,N+1} &= X^p_{N,N} + \alpha X^p_{N-1,N} \qquad \text{for} \quad 1 \leqslant p \leqslant N-1 \end{aligned} \tag{2.11}$$

with the initial condition

$$X^p_{N,p+1} = \alpha\beta Y_{N-1,p+1} \qquad \text{for} \quad 1 \leqslant p \leqslant N \tag{2.12}$$

where we used the extended definitions $Y_{0,1}$ and $Y_{N,N+2}$ of the $Y_{N,K}$. Solving these recursion relations gives the exact average occupation numbers $\langle \tau_i \rangle$ through Eqs. (2.3), (2.7), and (2.8). This was done in ref. 1 for $\alpha = \beta = 1$. Here we present the solution for arbitrary α and β.

For a solution of these recursion relations and initial conditions define the functions $G^M_{N,K}(x)$ by

$$G^M_{N,K}(x) = \sum_{r=0}^{M-1} b_{N,K}(r)\, x^r \qquad (N \geqslant 1) \tag{2.13}$$

with

$$b_{N,K}(r) = \binom{K-2+r}{K-2} - \binom{K-2+r}{N} \tag{2.14}$$

For later convenience also define $b_{0,1}(0) = G_{0,0}^1 = G_{0,1}^1 = 1$. As a result of the symmetries of the coefficients $b_{N,K}(r)$ these functions satisfy various relations given in the Appendix. In particular, from the recursion relations (A.3) and the special values (A.4) one can show that the quantity

$$Y_{N,K}(\alpha, \beta) = \beta^N G_{N,K}^N(\alpha) + \sum_{s=0}^{K-2} \alpha^{N-s} \beta^{N-K+1+s} G_{N,N}^{s+1}(\alpha) \tag{2.15}$$

solves the recursion relations (2.9) with the initial conditions (2.10).

Relations (2.11) with initial condition (2.12) are satisfied by

$$\begin{aligned} X_{N,K}^p(\alpha, \beta) = {} & \sum_{r=0}^{N-p} b_{N-p,K-p}(r)\, \alpha^{r+1} \beta^{r+1} Y_{N-r-1,p+1}(\alpha, \beta) \\ & + \beta^{N-K+2} \sum_{r=0}^{K-p-2} \alpha^{N+1-p-r} G_{N-p,N-p}^{K-p-1-r}(\beta)\, Y_{p-1+r,p+1}(\alpha, \beta) \end{aligned} \tag{2.16}$$

Using the first of equations (A.4), one obtains from this

$$Z_N = Y_{N,N+1} = \sum_{s=0}^{N} \beta^s \alpha^{N-s} G_{N,N}^{s+1}(\alpha) \tag{2.17}$$

and after some computation, involving relabeling of indices, we get

$$T_{N,p} = X_{N,N+1}^p = \alpha\beta \sum_{s=0}^{N-p} \alpha^s G_{N-p,N-p}^{s+1}(\beta)\, Y_{N-s-1,p+1}(\alpha, \beta) \tag{2.18}$$

This expression is exact for any $N \geq 1$, $1 \leq p \leq N$. Substitution in (2.3) gives the exact density profile for arbitrary α and β.

Equations (2.17) and (2.18) provide also an exact expression for the conserved current $j = \langle \tau_i \rangle - \langle \tau_i \tau_{i+1} \rangle = \text{const}$, and consequently for the correlation function $\langle \tau_i \tau_{i+1} \rangle$. To see this, note that taking $i = N$, one obtains $\langle \tau_N \tau_{N+1} \rangle = (1-\beta) \langle \tau_N \rangle$, since site $N+1$ represents the reservoir of constant density $1-\beta$. Therefore one has[1]

$$j = \beta \langle \tau_N \rangle \tag{2.19}$$

On the other hand, taking $i = 0$, one gets $\langle \tau_0 \tau_1 \rangle = \alpha \langle \tau_1 \rangle$, since site 0 is the reservoir of constant density α. Thus we also have[1]

$$j = \alpha(1 - \langle \tau_1 \rangle) \tag{2.20}$$

Since, however, our exact result yields $\langle \tau_i \rangle$ for any i, we can calculate the exact current j, and hence $\langle \tau_i \tau_{i+1} \rangle$.

3. DISCUSSION OF THE DENSITY PROFILE

In order to analyze the density, it is convenient to study the quantity

$$t_N(p) = (T_{N,p+1} - T_{N,p})/Z_N \tag{3.1}$$

which becomes the spatial derivative of the density profile in the continuum limit. It turns out to be given by ($p \neq N$)

$$t_N(p) = (1-\alpha-\beta)\,\beta^p G^{N-p}_{N-p,N-p}(\beta)\,\alpha^{N-p} G^p_{p,p}(\alpha)/Z_N \tag{3.2}$$

which for $\alpha \neq 1-\beta$ can be more conveniently written in the form

$$t_N(p) = F_p(\alpha)\,F_{N-p}(\beta)/\tilde{Z}_N \tag{3.3}$$

with

$$F_N(x) = x^{-N-1} G^N_{N,N}(x) \tag{3.4}$$

and

$$\tilde{Z}_N = \frac{Z_N}{(1-\alpha-\beta)\,\alpha^{N+1}\beta^{N+1}} = \begin{cases} \dfrac{F_N(\beta)-F_N(\alpha)}{\alpha(1-\alpha)-\beta(1-\beta)}, & \alpha \neq \beta, \quad 1-\beta \\[2ex] -\dfrac{F'_N(\beta)}{1-2\beta}, & \alpha = \beta \neq \dfrac{1}{2} \end{cases} \tag{3.5}$$

where the prime denotes the derivative with respect to β. The last of the two equations (3.5) can be obtained by changing the order of summation in (2.17).

For $\alpha = 1-\beta$ one obtains directly from (3.2) that $t_N(p) = 0$, i.e., the profile is constant on this curve. This result was already obtained in ref. 1. From (3.3) we learn that up to the amplitude $\tilde{Z}$, the derivative $t(p)$ of the density profile can be written as a product of two functions; one of α and the other of β: $t_N(p) \propto F_p(\alpha)\,F_{N-p}(\beta)$.

This fact has important and surprising consequences. It clearly implies that phase transitions (i.e., nonanalytic changes in the p dependence of the density profile) can occur on two kinds of lines: $\alpha = \alpha_c$ and *any* β, or $\beta = \beta_c$ and *any* α. Hence if a phase transition is predicted to occur on the $\beta > 1/2$ segment of the line $\alpha = 1/2$ (the mean-field transition to the maximal current phase), then the transition *must* extend to the $\beta < 1/2$ regime as well! This means that instead of a single high-density phase B predicted by mean field there are in fact two such phases. Indeed, analysis of the func-

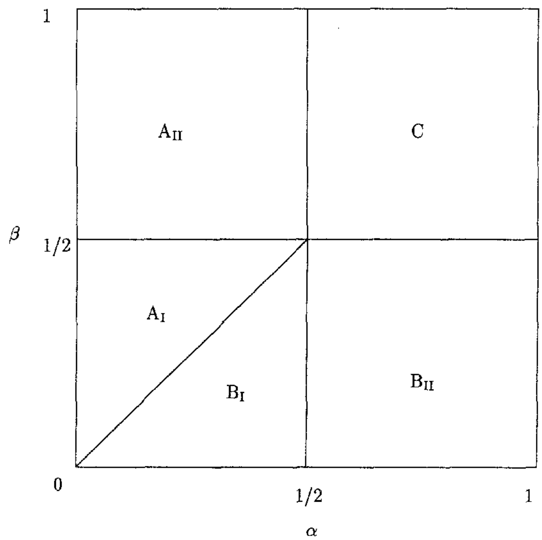

Fig. 2. Exact phase diagram of the model in the α–β plane. The low (high) density phase shown in Fig. 1 is divided into two phases, A_{I} and A_{II} (B_{I} and B_{II}) along the curve $\beta = 1/2$ ($\alpha = 1/2$).

tion $F_p(x)$, presented below, reveals that its dependence on p changes at $x = 1/2$. Similar considerations hold for the line $\beta = 1/2$ and $\alpha < 1/2$, which separates the low-density phase A into two distinct phases (Fig. 2). These new transitions were not found by the mean-field calculation.

Another unexpected consequence of the separability into a product is the existence of *two* independent length scales in the model, one determined by the injection rate α, the other one by the absorption rate β. This is surprising, as one might believe that only the larger of these two quantities determines the behavior of the system. In fact, as long as the system is not in the maximal current phase, this indeed is the case as far as the current $j = \langle \tau_i \rangle - \langle \tau_i \tau_{i+1} \rangle$ is concerned: In the continuum limit one has $j = \beta(1-\beta)$ for $\alpha > \beta$ and $\beta < 1/2$, and $j = \alpha(1-\alpha)$ for $\beta > \alpha$ and $\alpha < 1/2$ (whereas $j = 1/4$ if both α and β are larger than 1/2). Since in the mean-field calculation the shape of the density profile is determined by only the current, phase transitions are seen neither at $\alpha = 1/2$ and $\beta < 1/2$, not at $\beta = 1/2$ and $\alpha < 1/2$. Prior to presenting an explanation for the unexpected existence of the additional phases and phase transitions, we study the density profile in the thermodynamic limit $N \to \infty$.

4. DENSITY PROFILE IN THE LARGE-N LIMIT

We want to discuss the density profile of a large system ($N \gg 1$) as a function of the space coordinate p at large distances from both ends, i.e., we consider $p \gg 1$ and $r = N - p \gg 1$. So we need an asymptotic expression for $F_L(x)$ for large L. Splitting $F_L(x)$ into two pieces $F_L^{(1)}(x)$ and $F_L^{(2)}(x)$ as in Eq. (A.11) allows for an expansion in $1/L$. For $x < 1/2$ the dominating contribution is $F_L^{(1)}$, since $F_L^{(2)}/F_L^{(1)} \propto \exp(-aL)$ with some constant a:

$$F_L(x) = \frac{1-2x}{[x(1-x)]^{L+1}}\,[1 + O(e^{-aL})], \qquad x < \frac{1}{2} \tag{4.1}$$

If $x > 1/2$, then $F_L^{(1)} = 0$ and up to order $1/L$

$$\begin{aligned} F_L(x) &= \frac{c_L}{(1-2x)^2}\,[1 + O(L^{-1})] \\ &= \frac{4^L}{(1-2x)^2\sqrt{\pi}\,L^{3/2}}\,[1 + O(L^{-1})], \qquad x > \frac{1}{2} \end{aligned} \tag{4.2}$$

This expression diverges for $x \to 1/2$. For $x = 1/2$ one obtains [see (A.14)]

$$F_L(x) = 2\,\frac{4^L}{(\pi L)^{1/2}}\,[1 + O(L^{-1})] \tag{4.3}$$

Using the expansions (4.1)–(4.3) and the expression (3.5) for the normalization $\tilde{Z}_N$, one can compute the shape of the density profile given by $t_N(p)$. We define a length scale ξ_σ by

$$\xi_\sigma^{-1} = -\log[4\sigma(1-\sigma)] \tag{4.4}$$

As σ reaches $1/2$, ξ_σ diverges. For the various phases A_{I}–C (Fig. 2) one finds in the large-N limit (such that $1 \ll p$, $1 \ll N - p$, i.e., p is far from both ends of the system) the following results.

4.1. High-Density Phase B_{I}

This phase is defined by the region $\beta < \alpha < 1/2$. From the expansion (4.1) one finds an exponential decay of the density profile with length scale $\xi^{-1} = \xi_\alpha^{-1} - \xi_\beta^{-1}$,

$$\begin{aligned} t_N(p) &= (1-2\alpha)\left(1 - \frac{4\beta(1-\beta)}{4\alpha(1-\alpha)}\right)\left(\frac{4\beta(1-\beta)}{4\alpha(1-\alpha)}\right)^p \\ &= (1-2\alpha)\left(1 - \frac{4\beta(1-\beta)}{4\alpha(1-\alpha)}\right)e^{-p/\xi} \end{aligned} \tag{4.5}$$

The density approaches its bulk value $\rho_{\text{bulk}} = 1 - \beta$ from below. One has $j = \beta(1-\beta)$ and from (2.20), $\langle \tau_1 \rangle = 1 - \beta(1-\beta)/\alpha < 1 - \beta = \langle \tau_N \rangle$.

4.2. Transition Line from High-Density Phase B_{I} to High-Density Phase B_{II}

On approaching $\alpha = 1/2$ from below in the region $\beta < 1/2$, we find that ξ_α diverges but ξ_β remains finite. For $\alpha = 1/2$ the slope of the profile is of the form

$$t_N(p) \sim p^{-z_\alpha} e^{-p/\xi_\beta} \tag{4.6}$$

The values of the length scale ξ_β and the exponent z_α can be read off the exact expression (4.3), which for large N becomes

$$\begin{aligned} t_N(p) &= \frac{(1-2\beta)^2}{2\sqrt{\pi}} \frac{[4\beta(1-\beta)]^p}{p^{1/2}} \\ &= \frac{(1-2\beta)^2}{2\sqrt{\pi}} p^{-1/2} e^{-p/\xi_\beta} \end{aligned} \tag{4.7}$$

The current and the boundary values are given by the same expressions as in the high-density phase I.

4.3. High-Density Phase B_{II}

On crossing the phase transition line into the high-density phase B_{II} defined by $\alpha > 1/2$ and $\beta < 1/2$, the decay exponent changes to $z_\alpha = 3/2$ [see Eq. (4.2)] and one obtains

$$\begin{aligned} t_N(p) &= \frac{(1-\alpha-\beta)(\alpha-\beta)}{(1-2\alpha)^2 \sqrt{\pi}} \frac{[4\beta(1-\beta)]^p}{p^{3/2}} \\ &= \frac{(1-\alpha-\beta)(\alpha-\beta)}{(1-2\alpha)^2 \sqrt{\pi}} p^{-3/2} e^{-p/\xi_\beta} \end{aligned} \tag{4.8}$$

The current and the boundary values are given by the same expressions as in the high density phase I, but note that the slope of the profile changes sign on the curve $\alpha = 1 - \beta$. Along this curve the density is constant, $\langle \tau_i \rangle = \rho_{\text{bulk}} = 1 - \beta$ for $1 \leqslant i \leqslant N$. For $\alpha > 1 - \beta$ the slope is negative.

4.4. Transition from High-Density Phase B_{II} to the Maximal Current Phase C

When β reaches the critical value 1/2 in the region $\alpha > 1/2$ and $\beta \leqslant 1/2$, then also ξ_β diverges and the slope of the profile is given by

$$t_N(p) = -\frac{1}{4\sqrt{\pi}}\left(1-\frac{p}{N}\right)^{-1/2} p^{-3/2} \tag{4.9}$$

Near the origin ($1 \ll p \ll N$) we can neglect the piece with p/N in (4.9), so the slope is dominated by p^{-z_α} with $z_\alpha = 3/2$. In the boundary region ($p = N - r$, $1 \ll r \ll N$) the shape of the profile is determined by r^{-z_β} with $z_\beta = 1/2$, but the amplitude of $t_N(r)$ is only of order $1/N$. Therefore, up to corrections of order $1/N$, the profile near the boundary is flat, whereas it decays as $p^{-1/2}$ with the distance p from the origin to its bulk value $\rho_{\mathrm{bulk}} = 1/2$. The current reaches its maximal value $j = 1/4$ and one finds $\langle \tau_N \rangle = \rho_{\mathrm{bulk}} = 1/2$ and $\langle \tau_1 \rangle = 1 - 1/(4\alpha)$.

4.5. Maximal Current Phase

If $\beta > 1/2$ and $\alpha > 1/2$, the derivative $t_N(p)$ depends neither on α nor on β. Near the origin and near N the slope of the profile is determined by $z_\alpha = z_\beta = 3/2$:

$$t_N(p) = -\frac{1}{4\sqrt{\pi}}\left(1-\frac{p}{N}\right)^{-3/2} p^{-3/2} \tag{4.10}$$

Therefore the density approaches its bulk value $\rho_{\mathrm{bulk}} = 1/2$ as $p^{-1/2}$ with the distance p from the origin from above and as $r^{-1/2}$ with the distance $r = N - p$ from the boundary from below. The current takes its maximal value $j_{\max} = 1/4$ throughout the phase and one obtains $\langle \tau_N \rangle = 1/(4\beta)$ and $\langle \tau_1 \rangle = 1 - 1/(4\alpha)$.

4.6. Low-Density Phase A_{I}

This phase is defined by $\alpha < \beta < 1/2$ and is related to the high-density phase B_{I} by a particle–hole symmetry and therefore the decay is exponential. One finds

$$\begin{aligned} t_N(p) &= (1-2\beta)\left(1-\frac{4\alpha(1-\alpha)}{4\beta(1-\beta)}\right)\left(\frac{4\alpha(1-\alpha)}{4\beta(1-\beta)}\right)^{N-p} \\ &= (1-2\beta)\left(1-\frac{4\alpha(1-\alpha)}{4\beta(1-\beta)}\right) e^{-r/\xi} \end{aligned} \tag{4.11}$$

with a length scale $\xi^{-1}=\xi_{\alpha}^{-1}-\xi_{\beta}^{-1}$ and $r=N-p\gg 1$. The density approaches its bulk value $\rho_{\text{bulk}}=\alpha$ from above. The current is given by $j=\alpha(1-\alpha)$ and therefore, according to (2.19), $\langle\tau_N\rangle=\alpha(1-\alpha)/\beta>\alpha=\langle\tau_1\rangle$.

4.7. Low-Density Phase A_{II}

The profile in this regime ($\beta>1/2$, $\alpha<1/2$) is obtained from (4.8) by exchanging α and β and substituting p by $r=N-p$. This is a result of the particle–hole symmetry of the model. In the same way one obtains the profile on the phase transition lines from A_{I} to A_{II} and from A_{II} to C out of the profiles on the phase transition lines from B_{I} to B_{II} and B_{II} to C, respectively.

4.8. Coexistence Line

If $\alpha=\beta<1/2$, both ξ_α and ξ_β are finite, but since $\xi_\alpha=\xi_\beta$, one gets $\xi^{-1}=0$. As a result one finds a linear profile with a positive slope

$$t_N(p)=(1-2\alpha)/N \tag{4.12}$$

The current is given by $j=\alpha(1-\alpha)$ and one has $\langle\tau_1\rangle=\alpha$ and $\langle\tau_N\rangle=1-\alpha$.

5. DISCUSSION OF THE PHASE DIAGRAM

We turn now to discuss the various phases and the transitions between them on a more physical, intuitive basis. First we consider the case $\beta=1$. This situation corresponds to connecting the system to a reservoir of fixed density $\rho_0=\alpha$ at the origin, and another "reservoir" with $\rho_{N+1}=1-\beta=0$ at the boundary. We will consider the limit $N\to\infty$, and ask what are the possible steady-state density profiles that the system can have, and which interpolate between the two limiting values ρ_0 and ρ_{N+1}.

Let us start with $\alpha<1/2$, and try a density profile (a) that approaches (for $1\ll x\ll N$) a constant bulk value $\rho<\alpha$, before it decays to $\rho_{N+1}=0$. We now show that such a profile *cannot* be a steady state. To see this, note that in a bulk region with constant density there are no correlations (the steady state factorizes into a product measure) and therefore the current in the bulk is given by $j=\rho(1-\rho)$; whereas at the origin it is $j_0=\alpha(1-\rho_1)$, where ρ_1, the density at $x=1$, satisfies $1/2>\alpha\geqslant\rho_1\geqslant\rho$. If we can show that $j_0>j$, particles accumulate between the origin and the bulk, and hence the density is not stationary. Clearly, for $\rho_1=\rho$ we have $j_0=\alpha(1-\rho)>\rho(1-\rho)=j$, since $\alpha>\rho$. On the other hand, for $\rho_1=\alpha$ we have $j_0=$

$\alpha(1-\alpha) > \rho(1-\rho) = j$ for $1/2 > \alpha > \rho$. Hence $j_0 > j$ at the two endpoints of the interval $[\rho, \alpha]$ to which ρ_1 is limited; and since j_0 is a linear function of ρ_1, we must have $j_0 > j$ for the entire interval.

A different possible steady state profile (b) is one with $\alpha < \rho < 1/2$. Here we can show that $j_0 = \alpha(1-\alpha) < \rho(1-\rho) = j$: Under the present assumptions the density first interpolates between α and ρ, and hence $\alpha < \rho_1 < \rho$, and, as before, the relationship we wish to prove holds at both endpoints of this interval. If this holds, however, more particles leave the bulk than enter it, and ρ must decrease. Thus also (b) cannot be a steady state.

The last possibility of the kind considered, (c), has $\rho > 1/2 > \alpha$; we will return to this case later and show that for the presently used values of α and β it cannot be a steady-state profile either. The only remaining situation is the one in which $\rho = \alpha$. Then, obviously, $j_0 = \alpha(1-\alpha) = j$. Hence the bulk steady-state density must equal that of the reservoir.

The assumption $\alpha < 1/2$ was crucial for our proof of this fact, which is no longer true if $\alpha > 1/2$. In that case the bulk density is, independently of α, given by $\rho = 1/2$. To see this, we again assume all other possible values for the bulk steady-state density and rule out every other scenario. Let us start by assuming a decay to a bulk value $\rho < 1/2 (a')$; since, supposedly, we are in a steady state, we can choose some point i at which $1/2 > \rho_i > \rho$ as a new initial point of fixed density $\alpha' = \rho_i$; α' plays now the role of $\alpha < 1/2$ of the previously discussed situation (a), which, as we have shown, cannot be a steady state. Another possibility (b') has $\alpha > \rho > 1/2$. In this case we recall that near N the density profile must go from ρ to $\rho_{N+1} = 0$. To rule this out, we view the site $N+1$ as a reservoir of *holes* of fixed density 1. The bulk with $\rho > 1/2$ corresponds to hole density $\rho_h = 1 - \rho < 1/2$; holes move to the left, and if we exchange the roles of holes and particles, this situation becomes precisely the case (a') discussed above. Hence (b') is not possible either.[4]

We have just shown that for $\alpha > 1/2$ no steady state is possible with either bulk density $\rho < 1/2$ or $\rho > 1/2$; hence the only possibility left is $\rho_{\text{bulk}} = 1/2$. That is, for $\alpha > 1/2$ the bulk density is that one which supports the maximal current, irrespective of α, the density of the reservoir. This explains the transition observed at $\alpha = 1/2$, from a low-density phase with $\rho_{\text{bulk}} = \alpha$ to the maximal current phase, in which $\rho_{\text{bulk}} = 1/2$.

For the sake of convenience we limited the previous discussion to the $\beta = 1$ line. We now show that the transition survives when we move off this line. Of the cases discussed above, (a), (b), and (a') were ruled out with no

[4] Note that the situation (c) of the $\alpha < 1/2$ case, to which we promised to return, also requires that ρ goes from $\rho > 1/2$ to $\rho_{N+1} = 0$, and therefore is ruled out in the same way as (b').

mention of the fact that $\beta = 1$. In case (b') [and its equivalent, case (c)], we used a particle–hole symmetry to map the situation onto case (a'). Since there we had $\alpha > 1/2$, the same argument goes through for holes if $\beta > 1/2$; hence the same considerations give rise to the same phases as were obtained on the $\beta = 1$ line. This completes the picture for the regions $1/2 < \beta \leqslant 1$, and by particle–hole symmetry, for $1/2 < \alpha \leqslant 1$ as well.

Note that in the low-density phase A_{II} with $\rho_{\mathrm{bulk}} = \alpha$ the slope of the density profile changes sign on the curve $\alpha = 1 - \beta$. This can be understood as follows. The probability that a particles moves in the bulk (its average velocity) is $v = 1 - \alpha$, while the probability that it moves at the boundary is $v_N = \beta$. If $\beta > 1 - \alpha$, then $v_N > v$ and the system becomes depleted near the boundary because the current $j = \rho v$ is conserved. This corresponds the negative slope of the profile in this regime. On the other hand, if $\beta < 1 - \alpha$, one has $v_N < v$ and particles pile up. This leads to a positive slope. In the high-density phase B_{II} one finds the same result when compairing the velocity $v_0 = 1 - \alpha$ at the origin with the bulk velocity $v = \beta$.

Next, we discuss the low-density phase A_{I}, the high-density phase B_{I} in the region $0 < \alpha$, $\beta < 1/2$, and the transition between them. The bulk values in both phases and the slope of the profile can be derived in the same way as for the phases A_{II} and B_{II}. Note that in both phases one has $v_0 = 1 - \alpha > \beta = v_N$ and therefore the slope is always positive (particles pile up). The current is given by

$$j = \min(\alpha(1-\alpha), \beta(1-\beta)) \tag{5.1}$$

In order to understand the shape of the profile in phases A_{I} and B_{I} we assume that it is built up by a superposition of profiles with a constant density α up to some point x_0, followed by constant density $1 - \beta$. We call this sudden increase of the average density a domain wall[5] since it separates a region of high density $1 - \beta$ from a region of low density α. The picture we have in mind for this scenario is that particles injected with rate α at the origin move with constant average velocity $1 - \alpha > 1/2$ until they hit the domain wall, where they get stuck and continue to move only with velocity $\beta < 1/2$. This region of high density is caused by the blockage introduced through the connection to the reservoir of density $1 - \beta$ at the boundary. Such a scenario is plausible, since constant densities $\alpha < 1/2$ starting from the origin and $1 - \beta > 1/2$ connected to the boundary are both stable situations of the system as discussed above. The probability $p(x) \propto \exp(-x/\xi)$ of finding this domain wall at position x is determined by the length scale ξ given by $\xi^{-1} = \xi_\alpha^{-1} - \xi_\beta^{-1}$ [see (4.5) and (4.11)]. If $\alpha < \beta$

[5] We assume the width of this domain wall to be very small compared to the size of the system.

(low-density phase) then particles are absorbed with a higher probability than they are injected and the probability of finding the domain wall decreases exponentially with increasing distance $r = N - x$ from the boundary. On the other hand, in the case where $\alpha > \beta$ (high-density phase) the situation is reversed and $p(x)$ decreases with increasing distance from the origin. Averaging over all such profiles with the weight $p(x)$ leads to the observed exponential decay to the respective bulk value. This picture provides also a natural explanation of the linear profile on the transition line $\alpha = \beta$ where the absorption and injection probabilities are equal. Here ξ diverges and the probability of finding the domain wall at x is independent of x. Averaging over step functions with an equal weight for every position of the step clearly gives a linear profile. It is worth noting that the mean-field calculation done in ref. 1 gives a correct description of the phases A_{I} and B_{I}, but it singles out the constituent step function with the domain wall located in the center as the profile on the phase transition line. We should mention that this analysis, in particular the use of the domain wall picture for a description the two phases and the phase transition line, is based on our studies of a similar exclusion process with open boundary conditions but parallel dynamics.[9] For this model we found phases of type A_{I} and B_{I} and a phase transition separating them as in the system with sequential dynamics studied here. A careful study of the equal-time correlation functions leads to our interpretation in terms of domain walls. As the transition lines to the phases A_{II} or B_{II} are approached, this picture becomes invalid.

Finally we briefly discuss the phase transition from the high-density phase B_{I} to the high-density phase B_{II}. On approaching $\alpha = 1/2$ (but $\beta < 1/2$) the length scale ξ_α diverges while ξ_β remains finite. As a result neither the bulk density nor the way in which the bulk density is approached depends on α (except for the trivial fact that the density at the origin and consequently the amplitude of the derivative of the profile depend on α). The decay to the bulk density $\rho_{\mathrm{bulk}} = 1 - \beta$ is determined by ξ_β alone. Similarly the current does not depend on α, being $j = \beta(1 - \beta)$. A description of phase B_{II} also in terms of constituent profiles is appealing at first sight, but it is less convincing since a constant profile of density $\alpha > 1/2$ at the origin is *not* a stable situation. In order to get a more intuitive insight regarding this phase transition, we consider again the transition from the low-density phase A_{II} to the maximal current phase on the line $\alpha = 1/2$ but $\beta > 1/2$. In the maximal current phase C the bulk density and the way in which it is approached do not depend on α, whereas in the low-density phase A_{II}, α does determine the bulk density and how the profile decays to it. This is obviously due to the fact that if $\alpha > 1/2$, the particles close to the origin block each other rather than flowing away. As a result, the information corresponding to a change in the injection rate does not penetrate into the system. Clearly this description of the effect of α increasing beyond 1/2 on the transition from the low-density phase $A_{\rm I}$ to the maximal current phase does not depend on the absorption at the boundary and is therefore also applicable to the transition from phase $B_{\rm I}$ to phase $B_{\rm II}$.[6]

We conclude that the phase transitions to the maximal current phase from the phase $A_{\rm II}$ (or $B_{\rm II}$) are of the same nature as the phase transition from $B_{\rm I}$ to $B_{\rm II}$ (or from $A_{\rm I}$ to $A_{\rm II}$). These transitions are caused by reaching the maximal transport capacity of the system at the origin (or boundary) and result in the divergence of the corresponding length scale determining the shape of the profile. Note that in our explanation it was necessary to take into account local correlations rather than only the current. This is the reason why these phase transitions are not found in the mean-field calculation.

As opposed to these transitions, the one at $\alpha=\beta$ that takes the system from the low-density phase $A_{\rm I}$ to the high-density phase $B_{\rm I}$ is caused by the building up of domain walls. Such a wall is generated by the inhomogeneity forced on the system by being connected to two reservoirs of different densities. At the transition line the wall can be anywhere with equal probability. The "coexistence" of low- and high-density regions is known to occur also in other systems with such an inhomogeneity.[6,7,9,10]

APPENDIX. SOME USEFUL IDENTITIES FOR THE *G*-FUNCTION

The function $G^M_{N,K}(x)$ was defined in Eq. (2.13) as

$$G^M_{N,K}(x)=\sum_{r=0}^{M-1} b_{N,K}(r)\,x^r \qquad (N\geqslant 1) \tag{A.1}$$

with

$$b_{N,K}(r)=\binom{K-2+r}{K-2}-\binom{K-2+r}{N} \tag{A.2}$$

Furthermore, we defined $b_{0,1}(0)=G^1_{0,0}=G^1_{0,1}=1$. Using the symmetries of the coefficients $b_{N,K}(r)$, it is easy to prove the following recursion relations:

$$\begin{aligned}
G^M_{N,K}(x)&=G^M_{K-1,K}(x)+xG^{M-1}_{N,K+1}(x) &\qquad (2\leqslant K\leqslant N+1)&\\
G^N_{N,K}(x)&=G^N_{N,K-1}(x)+xG^{N-1}_{N-1,K}(x) &\qquad (2\leqslant K\leqslant N+1)&\qquad \text{(A.3)}\\
G^M_{N,N}(x)&=G^M_{N-1,N-1}(x)+xG^{M-1}_{N,N}(x) &\qquad (N\geqslant 2)&
\end{aligned}$$

[6] As a result of the particle–hole symmetry of the problem, the discussion of the transition from the low-density phase $A_{\rm I}$ to the low-density phase $A_{\rm II}$ proceeds along analogous lines.

One also finds

$$\begin{aligned} &G^{N}_{N,N}(x)=G^{N}_{N,N+1}(x)=G^{N+1}_{N,N}(x)=G^{N+1}_{N,N+1}(x) \qquad (N\geqslant 1)\\ &G^{0}_{N,K}(x)=G^{M}_{N,N+2}(x)=0 \qquad\qquad (A.4)\\ &G^{1}_{N,K}(x)=G^{M}_{N,1}(x)=1 \qquad (K, M\leqslant N+1) \end{aligned}$$

Equations (A.3) and (A.4) are necessary to prove that the function $Y_{N,K}(\alpha, \beta)$ and $X^{p}_{N,K}(\alpha, \beta)$ satisfy the recursion relations and initial conditions (2.9)–(2.12).

$G^{M}_{N,K}(x)$ can be expressed in terms of incomplete β functions:

$$(1-x)^{K-1}\, G^{M}_{N,K}(x)=I_{1-x}(K-1, M) - \left(\frac{x}{1-x}\right)^{N-K+2} I_{1-x}(N+1, M-N+K-2) \quad (A.5)$$

[This is a direct consequence of the definition of $I_x(P, Q)$.] From this expression one obtains

$$\begin{aligned} &(1-x)^{N+1}\, G^{M}_{N,K}(x)-x^{M}G^{N+1}_{M-1,M-N+K-1}(1-x)\\ &\quad=(1-x)^{N-K+2}-x^{N-K+2} \end{aligned} \quad (A.6)$$

and by setting $M=N$ and $M=N+1$,

$$G^{N+2}_{N,K}(x)=(1-x)\, G^{N+1}_{N+1,K+1}(x) \qquad (2\leqslant K\leqslant N+1) \quad (A.7)$$

From this relation one can see that relations (A.3) are consistent for $M=N=K$.

In the expression (3.3) for the density profile only the function $G^{L}_{L,L}(x)$ appears. From Eq. (A.7) one finds

$$G^{L}_{L,L}(x)=(1-x)\, G^{L+1}_{L+1,L+1}(x)+c_L x^{L+1} \quad (A.8)$$

with

$$c_L=-b_{L,L}(L+1)=\frac{(2L)!}{L!\,(L+1)!} \quad (A.9)$$

Defining $F_L(x)=x^{(-L-1)}G^{L}_{L,L}(x)$, one gets

$$F_L(x)=\frac{1-x}{[x(1-x)]^{L+1}}-\sum_{k=0}^{L-1} c_k[x(1-x)]^{k-L} \quad (A.10)$$

Now we can reexpress $F_L(x)$ for $x \neq 1/2$ in terms of a hypergeometric function:

$$F_L(x) = \frac{(1-2x)\,\Theta(1-2x)}{[x(1-x)]^{L+1}} + \frac{c_L}{(1-2x)^2} F\left(1, \frac{3}{2}; L+2; \frac{-4x(1-x)}{(1-2x)^2}\right) = F_L^{(1)}(x) + F_L^{(2)}(x) \tag{A.11}$$

Here $\Theta(z)$ is the step function

$$\Theta(z) = \begin{cases} 1 & z > 0 \\ 0 & z < 0 \end{cases} \tag{A.12}$$

For large L the hypergeometric function $F(1, \frac{3}{2}; L+2; z)$ reduces to

$$F(1, \tfrac{3}{2}; L+2; z) = 1 + O(L^{-1}) \tag{A.13}$$

Special exact values of $F_L(x)$ are

$$F_L\left(\frac{1}{2}\right) = 2\binom{2L}{L} = \frac{2}{\sqrt{\pi}} \frac{4^L}{L^{1/2}} [1 + O(L^{-1})] \tag{A.14}$$

and

$$F_L(1) = c_L = \frac{4^L}{(2\pi)^{1/2} L^{3/2}} [1 + O(L^{-1})] \tag{A.15}$$

Note Added. After completion of this work we received a preprint by B. Derrida, M. R. Evans, V. Hakim, and V. Pasquier, who solved the same problem by a different method.

ACKNOWLEDGMENTS

We thank B. Derrida and D. Mukamel for useful discussions. This research was partially supported by the Deutsche Forschungsgemeinschaft and the U.S.–Israel Binational Science Foundation.

REFERENCES

1. B. Derrida, E. Domany, and D. Mukamel, *J. Stat. Phys.* **69**:667 (1992).
2. D. Kandel, E. Domany, and B. Nienhuis, *J. Phys. A* **23**:L755 (1990).
3. J. Krug and H. Spohn, in *Solids far from Equilibrium: Growth, Morphology and Defects*, C. Godreche, ed. (Cambridge University Press, Cambridge, 1991).

4. M. Kardar, G. Parisi, and Y. Zhang, *Phys. Rev. Lett.* **56**:889 (1986).
5. J. Krug, *Phys. Rev. Lett.* **61**:1882 (1991).
6. S. A. Janowsky and J. L. Lebowitz, *Phys. Rev. A* **45**:618 (1992).
7. G. Schütz, *J. Stat. Phys.* **71**:471 (1993).
8. B. Derrida and M. R. Evans, *J. Phys. (Paris)* **3**:311 (1993).
9. G. Schütz, *Phys. Rev. E* **47** (1993), (in press).
10. D. Kandel and D. Mukamel, Weizmann preprint.
11. K. Nagel and M. Schreckenberg, *J. Phys. (Paris)* **2**:2221 (1992).
12. L.-H. Gwa and H. Spohn, *Phys. Rev. Lett.* **68**:725 (1992); *Phys. Rev. A* **46**:844 (1992).